MIT Libraries | DSpace@MIT

MIT Open Access Articles

Nonlinear effects in steady radiating waves: An exponential asymptotics approach

Massachusetts Institute of Technology

Nonlinear effects in steady radiating waves: an exponential asymptotics approach

Takeshi Kataoka[a], T. R. Akylas[b,*]

[a]*Department of Mechanical Engineering, Kobe University, 1-1 Rokkodai, Nada, Kobe 657-8501, Japan*
[b]*Department of Mechanical Engineering, Massachusetts Institute of Technology, Cambridge, MA 02139, USA*

Abstract

An asymptotic study is made of nonlinear effects in steady radiating waves due to moving sources in dispersive media. The focus is on problems where the radiated waves have exponentially small amplitude with respect to a parameter $\mu \ll 1$, as for instance free-surface waves due to a submerged body in the limit of low Froude number. In such settings, weakly nonlinear effects (controlled by the source strength ε) can be as important as linear propagation effects (controlled by μ), and computing the wave response for $\mu, \varepsilon \ll 1$ may require exponential (beyond-all-orders) asymptotics. This issue is discussed here using a simple model, namely, the forced Korteweg–de Vries (fKdV) equation where μ is the dispersion and ε is the nonlinearity parameter. The forcing term $f(x)$ is assumed to be even and its Fourier transform $\hat{f}(k)$ to decay for $k \gg 1$ like $Ak^{\alpha}\exp(-\beta k)$, where A, α and $\beta > 0$ are free parameters. For this class of forcing profiles, the wave response hinges on beyond-all-orders asymptotics only if $\alpha > -1$, and nonlinear effects differ fundamentally depending on whether $\alpha > 0$, $\alpha = 0$ or $-1 < \alpha < 0$. Fur-

---

[*]Corresponding author.
  Email address: `trakylas@mit.edu` (T. R. Akylas)

thermore, the sign of the forcing amplitude parameter A is an important controlling factor of the nonlinear wave response. The asymptotic results compare favorably against direct numerical solutions of the fKdV equation for a wide range of μ and ε, in contrast to the linear wave response whose validity is rather limited.

1. Introduction

Radiation of steady wave patterns by moving sources is a prominent feature of wave propagation in various physical settings. In fluid media in particular, there is rich literature on steady patterns of free-surface and internal gravity waves induced by a moving localized pressure distribution and by flow over topography or past a submerged body. These wave phenomena are fundamental to geophysical flow modeling and ship hydrodynamics [1, 2]. The standard theoretical approach to steady-wave problems is based on the linearized equations of motion assuming infinitesimal disturbances, subject to radiation conditions that derive from group velocity considerations [3, 4].

However, even when the source strength ε is weak ($\varepsilon \ll 1$) so linearization is expected to be valid, nonlinear effects may still play an important part in the wave response. Such a situation arises when the response wavelength Λ is short relative to a characteristic length scale L of the source ($\mu = \Lambda/L \ll 1$) so the radiated waves have exponentially small amplitude with respect to μ. Computing the wave response for $\mu, \varepsilon \ll 1$ then may require exponential ('beyond-all-orders') asymptotics, and weakly nonlinear effects

2

(controlled by ε) can be as important as linear propagation effects (controlled by μ). This shortcoming of linearization was noted in free-surface flow past a submerged body in the limit of low Froude number [5, 6] and later was studied via exponential asymptotics in a simple model problem [7].

The analysis in [7] considered the forced Korteweg–deVries (fKdV) equation in steady dimensionless form

$$\mu^2 u_{xx} + u - \varepsilon u^2 = f(x) \quad (-\infty < x < \infty),\tag{1.1}$$

subject to the radiation condition

$$u \to 0 \quad (x \to -\infty),\tag{1.2}$$

where the forcing term $f(x)$ is real and locally confined. Here, $\varepsilon \ll 1$ measures the strength of the forcing, and u has been scaled ($u \to \varepsilon u$) to make explicit that ε also controls the nonlinear term. In keeping with Eq. (1.2), waves may be radiated only downstream ($x \to \infty$) and they are expected to take the form

$$u \sim R \cos\left(\frac{x}{\mu} + \theta\right) \quad (x \to \infty),\tag{1.3}$$

where the amplitude R and the phase shift θ are to be determined. Thus, when the dispersion parameter $\mu \ll 1$ in Eq. (1.1), the response wavelength $2\pi\mu$ is short relative to the width of the forcing.

Owing to this lengthscale disparity, the Fourier transform of $f(x)$,

$$\hat{f}(k) = \frac{1}{2\pi} \int_{-\infty}^{\infty} f(x)\mathrm{e}^{-ikx}\mathrm{d}x,\tag{1.4}$$

at the response wavenumber $k = \pm 1/\mu$ is exponentially small with respect to μ (assuming $f(x)$ is analytic). This suggests that the response amplitude R is exponentially small as well, a claim also supported by the fact that

3

expanding u in powers of μ and ε,

$$u = f - \mu^2 f_{xx} + \varepsilon f^2 + \cdots , \tag{1.5}$$

shows no sign of radiating waves at any order of approximation. As explained in [7], this issue can be handled by working in the wavenumber domain where Eq. (1.1) transforms to

$$(1 - \mu^2 k^2)\hat{u}(k) - \varepsilon \int_{-\infty}^{\infty} \hat{u}(l)\hat{u}(k - l)\mathrm{d}l = \hat{f}(k). \tag{1.6}$$

The radiating wave in Eq. (1.3) is associated with the presence of simple-pole singularities of $\hat{u}(k)$ at $k = \pm 1/\mu$. Thus, the amplitude R and phase shift θ are found by computing the corresponding (exponentially small) residues asymptotically for μ, $\varepsilon \ll 1$ and then inverting the Fourier transform along an integration path consistent with the radiation condition (1.2).

This exponential asymptotics procedure was illustrated in [7] for $f(x) = \mathrm{sech}^2 x$, $\mathrm{sech}\, x$ and $\exp(-x^2)$. In these examples, the radiating waves, although they feature exponentially small amplitude in μ, $\varepsilon \ll 1$, are governed by a nonlinear beyond-all-orders generation mechanism. Furthermore, comparisons between theoretical predictions and numerical results indicate that this mechanism remains in control even for moderately small μ and ε, where the wave amplitude is substantial, so linearization has rather limited validity. In addition, the wavenumber procedure proposed in [7] was applied to internal gravity waves ('lee' waves) generated by stratified flow over topography with $\mathrm{sech}^2 x$ and $\mathrm{sech}\, x$ profile [8], and linearization was found to suffer similar limitations.

Later, the results obtained in [7] for $f(x) = \mathrm{sech}^2 x$ and $\mathrm{sech}\, x$ also were recovered using a nonlinear WKB technique that focuses on the singularities of expansion (1.5) in the complex plane [9]. A comprehensive discussion of

4

various beyond-all-orders techniques as applied to radiating waves is presented in [10], and a review of more recent advances is made in [11].

It is worth noting that the specific forcing profiles considered in [7 – 9] look similar in the physical domain; yet, their asymptotic treatments in the wavenumber domain are distinct. Furthermore, there are profound differences in how nonlinearity affects the radiating waves for each of these forcings [7 –11]. Thus, it is natural to ask: (i) what particular features of the forcing profile $f(x)$ are essential to the asymptotic analysis; and (ii) whether it is possible, instead of a case-by-case treatment, to set up a theory for radiating waves due to a broad class of sources.

The present article addresses these questions in the context of the fKdV equation (1.1), using the wavenumber exponential asymptotics approach. Specifically, the forcing term is taken to be real and even in x and its (real and even) Fourier transform is assumed to decay exponentially for large k, like

$$\hat{f}(k) \sim A\,|k|^{\alpha}\exp\left(-\beta\,|k|\right) \quad (|k| \to \infty), \tag{1.7}$$

where A, α and β are real and $\beta > 0$. This class of $f(x)$ includes as special cases the $\mathrm{sech}^2 x$, $\mathrm{sech}\,x$ and algebraically decaying profiles considered earlier [6 –11].

We find that for $\mu, \varepsilon \ll 1$ the radiating wave amplitude R and phase shift θ are controlled by a nonlinear beyond-all-orders mechanism only if $\alpha > -1$. Furthermore, the procedure for computing R and θ hinges on whether (i) $\alpha > 0$, (ii) $\alpha = 0$ or (iii) $-1 < \alpha < 0$. Specifically, for $\alpha > 0$, the residues of the simple poles of $\hat{u}(k)$ at $k = \pm 1/\mu$ (and hence R and θ) can be computed directly from a nonlinear Volterra-type integral equation that 'sums' to all orders the perturbation expansion (1.5), similar to the case

5

$\alpha = 1$ for $f(x) = \text{sech}^2 x$ considered in [7]. For $\alpha = 0$, this 'outer' analysis must be supplemented with an 'inner' analysis in the vicinity of the simple-pole singularities, as also found in [7, 11] for $f(x) = \text{sech}\, x$. Finally, for $-1 < \alpha < 0$, the outer and inner analyses are more involved than for $\alpha = 0$ because nonlinearity affects also the exponential factor in the expression for R.

In addition, the present study reveals that the sign of the forcing amplitude A (which scales out in the linear limit, $\varepsilon = 0$) is a major controlling factor of the nonlinear wave response. This point was not appreciated in prior work, which dealt with $A > 0$ only. The theoretical predictions are supported by numerical results for values of α representative of the regimes (i)–(iii) above and for a wide range of μ and ε. Overall, it is concluded that the linear wave response has rather limited validity.

Based on prior experience [8], it is expected that the methodology developed here for the fKdV equation will be applicable to steady radiating free-surface and internal gravity waves due to forcings (e.g., localized applied pressure or bottom topography) that satisfy the assumed asymptotic behavior of $\hat{f}(k)$ in Eq. (1.7). In particular, for $\alpha = 0$, this class of forcing profiles $f(x)$ is relevant to the classical problem of free-surface flow past a submerged circular cylinder [6].

2. Scalings

An advantage of working in the wavenumber domain is that the perturbation expansion of $\hat{u}(k)$ in powers of μ and ε becomes disordered for $|k| \gg 1$, which provides a hint of whether nonlinearity can affect the pole residues at $k = \pm 1/\mu$. Specifically, taking Fourier transform of expansion

6

(1.5) of $u(x)$ yields

$$\hat{u}(k) = \left\{1 + \mu^2 k^2 + \cdots\right\} \hat{f}(k) + \varepsilon \int_{-\infty}^{\infty} \hat{f}(l)\hat{f}(k-l)\mathrm{d}l + \cdots. \qquad (2.1)$$

Furthermore, making use of Eq. (1.7), the asymptotic behavior as $|k| \to \infty$ of the convolution integral above for $\widehat{f^2}$ is found to be

$$\widehat{f^2} \sim \begin{cases} A^2 c\,|k|^{2\alpha+1} \exp(-\beta\,|k|) & (\alpha > -1) \\[2mm] O\left(\,|k|^\alpha \exp(-\beta\,|k|)\,\right) & (\alpha < -1), \end{cases} \qquad (2.2)$$

where

$$c \equiv \int_0^1 \mathrm{d}p \; p^\alpha (1-p)^\alpha = \frac{\Gamma(\alpha+1)^2}{\Gamma(2\alpha+2)} \qquad (2.3)$$

and Γ denotes the gamma function. Thus, for $\varepsilon \ll 1$ nonlinearity can contribute to the disordering for $|k| \gg 1$ of expansion (2.1), only if

$$\alpha > -1. \qquad (2.4)$$

Assuming this condition is satisfied and making use of (1.7) and (2.2), expansion (2.1) takes the following form for $|k| \gg 1$

$$\hat{u} \sim A\,|k|^\alpha \left\{1 + \mu^2 k^2 + \varepsilon Ac\,|k|^{\alpha+1} + \cdots\right\} \exp(-\beta\,|k|). \qquad (2.5)$$

Based on Eq. (2.5), nonlinear effects are expected to come into play for k near the poles of $\hat{u}(k)$ at $k = \pm 1/\mu$, if $\varepsilon A = O(\mu^{\alpha+1})$. Accordingly, we set

$$\varepsilon = \mu^{\alpha+1}. \qquad (2.6)$$

This fixes ε in terms of μ, and A will serve as the second independent parameter in the fKdV equation: $|A| = O(1)$ controls the balance of nonlinearity with dispersion, while the sign of A specifies the polarity of the forcing term. Earlier work [7] also adopted (2.6) (with $\alpha = 1$ and $\alpha = 0$ for the $\mathrm{sech}^2 x$ and the $\mathrm{sech}\,x$ forcing, respectively) but A was fixed to $A = 1$.

7

3. Two-scale asymptotics in the wavenumber domain

3.1. Uniformly valid approximation of $\hat{u}(k)$

The disordering of expansion (2.1) for $|k| \gg 1$ noted above suggests a uniformly valid approximation of $\hat{u}(k)$ that combines: (i) the straightforward perturbation expansion (2.1), valid for $0 \leq |k| \ll 1/\mu$, with (ii) the two-scale expansion

$$\hat{u} \sim \frac{A}{\mu^\alpha} U(\kappa)\, e^{-\beta|k|} + \cdots, \tag{3.1}$$

valid for $\kappa = \mu k = O(1)$. Here, in analogy with 'two-timing' asymptotics, $U(\kappa)$ may be viewed as the 'slowly varying' amplitude of the 'fast' exponential $e^{-\beta|k|}$. Furthermore, in view of Eq. (2.5), we require that

$$U \sim |\kappa|^\alpha \left\{ 1 + \kappa^2 + Ac\,|\kappa|^{\alpha+1} + \cdots \right\} \quad (\kappa \to 0). \tag{3.2}$$

Thus, taking δ to be a constant such that $\mu \ll \delta \ll 1$, expansions (i) and (ii) match for k in the intermediate range

$$1 \ll |k| = O(1/\delta) \ll 1/\mu. \tag{3.3}$$

3.2. Integral equation for $U(\kappa)$

We now derive an approximate governing equation for $U(\kappa)$, $0 < \kappa = O(1)$. To this end, returning to Eq. (1.6), we write the convolution integral for $\widehat{u^2}$ as

$$\widehat{u^2} = 2 \int_{-\infty}^{k/2} \hat{u}(l)\hat{u}(k-l)\mathrm{d}l. \tag{3.4}$$

In this expression, as $k - l = O(1/\mu)$ for $\kappa = O(1)$, $\hat{u}(k-l)$ is replaced by the two-scale approximation (3.1),

$$\widehat{u^2} \sim 2\frac{A}{\mu^\alpha}\, e^{-\beta k} \int_{-\infty}^{k/2} \hat{u}(l)U(\kappa - \mu l)\, e^{\beta l}\mathrm{d}l. \tag{3.5}$$

8

For $-\infty < l \leq 0$, the main contribution to the integral above comes from $|l| = O(1)$ because $\hat{u}(l)\mathrm{e}^{\beta l}$ is exponentially small for $l \ll -1$; thus, $\hat{u}(l)$ is approximated by expansion (2.1): $\hat{u}(l) = \hat{f}(l) + \cdots$. In the rest of the integration range $(0 < l \leq k/2)$, since $k/2 = O(1/\mu)$, $\hat{u}(l)$ is approximated by expansion (2.1) for $0 \leq l \leq 1/\delta$, where $1 \ll 1/\delta \ll 1/\mu$ in keeping with (3.3), and by expansion (3.1) for $1/\delta \leq l \leq k/2$. Upon implementing these approximations in Eq. (3.5), we find

$$
\widehat{u^2} \sim 2\frac{A}{\mu^\alpha}\mathrm{e}^{-\beta k}\left\{ \frac{A}{\mu^{\alpha+1}} \int_{\mu/\delta}^{\kappa/2} U(\lambda)U(\kappa - \lambda)\mathrm{d}\lambda \right.
$$
$$
\left. + \int_{-\infty}^{1/\delta} \hat{f}(l)U(\kappa - \mu l)\mathrm{e}^{\beta l}\mathrm{d}l \right\}.
\tag{3.6}
$$

Finally, making use of Eqs. (1.7), (3.1) and (3.6), it follows from Eq. (1.6) that $U(\kappa)$ is governed by

$$
(1 - \kappa^2)U(\kappa) - 2A \int_{\mu/\delta}^{\kappa/2} U(\lambda)U(\kappa - \lambda)\mathrm{d}\lambda
$$
$$
- 2\mu^{\alpha+1} \int_{-\infty}^{1/\delta} \hat{f}(l)U(\kappa - \mu l)\mathrm{e}^{\beta l}\mathrm{d}l = \kappa^\alpha.
\tag{3.7}
$$

3.3. Overview of analytical procedure

Equation (3.7) forms the basis of the ensuing analysis. The goal is to compute the residues of the expected simple poles of $U(\kappa)$ at $\kappa = \pm 1$, which translate into simple poles of $\hat{u}(k)$ at $k = \pm 1/\mu$, and thereby determine the radiated waves upon inverting $\hat{u}(k)$. Of particular interest is how these residues are impacted by the two integrals in Eq. (3.7), which account for nonlinear effects in the radiated wave amplitude and phase. Formally, the first of these integrals dominates; however, for $-1 < \alpha \leq 0$, the second integral also comes into play when $\kappa = \pm 1 + O(\mu)$ and thus affects the pole residues. This necessitates an outer–inner matched asymptotics procedure, detailed below.

9

4. Outer equation

To leading order in μ and μ/δ, Eq. (3.7) reduces to

$$(1 - \kappa^2)U(\kappa) - 2A \int_0^{\kappa/2} U(\lambda)U(\kappa - \lambda)\mathrm{d}\lambda = \kappa^{\alpha}. \tag{4.1}$$

This Volterra-type integral equation is to be solved subject to the condition

$$U(\kappa) \sim \kappa^{\alpha} \quad (\kappa \to 0), \tag{4.2}$$

in keeping with (3.2).

We first examine the nature of the singularity of $U(\kappa)$ as $\kappa \to 1$ based on the 'outer' equation (4.1). The results of this outer analysis depend critically on whether $\alpha > 0$, $\alpha = 0$ or $-1 < \alpha < 0$, as discussed below.

4.1. Outer analysis for $\alpha > 0$

Under the condition $\alpha > 0$, the integral term in Eq. (4.1) is subdominant as $\kappa \to 1$, and $U(\kappa)$ features a simple pole at $\kappa = 1$ irrespective of A. This is deduced most easily by differentiating (4.1),

$$(1 - \kappa^2)U'(\kappa) - 2\kappa U(\kappa) - AU(\kappa/2)^2$$
$$- 2A \int_0^{\kappa/2} U(\lambda)U'(\kappa - \lambda)\mathrm{d}\lambda = \alpha\kappa^{\alpha-1}, \tag{4.3}$$

and applying dominant balance. Specifically, letting

$$U'(\kappa) \sim \frac{C}{(1-\kappa)^p}, \quad U(\kappa) \sim \frac{C}{(p-1)(1-\kappa)^{p-1}} \quad (\kappa \to 1), \tag{4.4}$$

with $p > 1$ and C constants, the first two terms in Eq. (4.3), which are $O(1-\kappa)^{1-p}$, dominate the integral term; in view of (4.2), the latter is $O(1-\kappa)^{1-p+\alpha}$ for $\alpha < p-1$ and $O(1)$ for $\alpha \geq p-1$. This dominant balance specifies $p = 2$, confirming that $U(\kappa)$ has a simple pole according to (4.4).

Returning to Eq. (3.7), the simple-pole singularity deduced above persists, as the $O(\mu^{\alpha+1}, \mu/\delta)$ correction terms remain relatively small as $\kappa \to 1$. Thus, for $\alpha > 0$, the outer analysis is sufficient to determine the pole residues of $\hat{u}(k)$ at $k = \pm 1/\mu$ and thereby compute the radiating waves downstream. The effect of nonlinearity is encapsulated in the value of the constant C in (4.4), which depends on A. Details are given in Section 5.

4.2. Outer analysis for $\alpha = 0$

An ansatz similar to (4.4) also works for $\alpha = 0$. However, now the integral in Eq. (4.3) participates in the dominant balance and the strength of the singularity, which no longer is a simple pole, depends on A. Specifically, substituting (4.4) in Eq. (4.3) and balancing the first two terms with the $O(1-\kappa)^{1-p}$ contribution of the integral, yields $p = 2 + A$. Therefore,

$$U'(\kappa) \sim \frac{C_1}{(1-\kappa)^{2+A}}, \quad U(\kappa) \sim \frac{C_1}{(1+A)(1-\kappa)^{1+A}} \quad (\kappa \to 1), \qquad (4.5)$$

where C_1 is a constant. It should be noted that the dominant balance above and the asymptotic behavior (4.5) are valid only if $p > 1$, i.e. $A > -1$.

For $A \leq -1$, the singularity of $U(\kappa)$ at $\kappa = 1$ is determined by further differentiating Eq. (4.3) and balancing the most singular terms. Specifically, for $-n < A \leq -n+1$, where $n \geq 2$ is integer, we differentiate Eq. (4.3) $n-1$ times,

$$(1 - \kappa^2)U^{(n)}(\kappa) - 2n\kappa U^{(n-1)}(\kappa) + \cdots$$
$$- 2A \int_0^{\kappa/2} U(\lambda)U^{(n)}(\kappa - \lambda)\mathrm{d}\lambda = 0. \qquad (4.6)$$

Then, upon substituting the ansatz $U^{(n)}(\kappa) \sim C_n/(1-\kappa)^p$ (with $p > 1$ and C_n constants) in Eq. (4.6) and balancing the first two terms with the integral

11

term, we find $p = 1 + n + A > 1$. Thus, for $-n < A \leq -n+1$, the singular behavior is

$$U^{(n)}(\kappa) \sim \frac{C_n}{(1-\kappa)^{1+n+A}}, \quad U^{(n-1)}(\kappa) \sim \frac{C_n}{(n+A)(1-\kappa)^{n+A}} \quad (\kappa \to 1). \tag{4.7}$$

The fact that the outer equation (4.1) predicts a singularity different from a simple pole suggests that a separate analysis based on Eq. (3.7) is needed in the vicinity of $\kappa = 1$. This 'inner' solution reveals the expected simple pole and enables computing the radiated waves downstream, as discussed in Section 6.

4.3. Outer analysis for $-1 < \alpha < 0$

In this instance, a power singularity similar to (4.4) does not work because the first two terms in Eq. (4.3) are subdominant relative to the integral term. Instead, after experimenting with various singularities stronger than a simple power, for $A > 0$, we try an exponential singularity combined with a power in the form

$$U(\kappa) \sim \frac{C_-}{(1-\kappa)^p} \exp\left(\frac{B}{(1-\kappa)^q}\right) \quad (\kappa \to 1), \tag{4.8}$$

where $q > 0$, $B > 0$, p and C_- are constants. Substituting this ansatz in Eq. (4.1), for $1 - \kappa \equiv \xi \to 0$, the dominant contribution to the integral term comes from the neighborhood of $\lambda = 0$. Specifically, using (3.2) and with the change of variable $\lambda = \xi\rho$,

$$I \equiv \int_0^{\kappa/2} U(\lambda)U(\kappa - \lambda)\mathrm{d}\lambda$$

$$\sim C_- \xi^{\alpha-p+1} \int_0^{\kappa/2\xi} \mathrm{d}\rho \, \frac{\rho^\alpha}{(1+\rho)^p} \left(1 + A c \, \xi^{\alpha+1}\rho^{\alpha+1} + \cdots\right) \exp\left(\frac{B}{\xi^q(1+\rho)^q}\right). \tag{4.9}$$

12

Next, employing Laplace's method [12], the integral above is evaluated asymptotically as $\xi \to 0$ ($\xi^{-q} \to \infty$) by expanding the integrand about $\rho = 0$, where the exponent attains its maximum, and integrating term-by-term from 0 to ∞. Finally, this yields

$$
I \sim \frac{C_-}{(qB)^{\alpha+1}} \xi^r \exp\left(\frac{B}{\xi^q}\right)
$$
$$
\times \left\{ \Gamma(\alpha+1) + \frac{A\,c\,\Gamma(2\alpha+2)}{(qB)^{\alpha+1}} \xi^{(\alpha+1)(1+q)} + \frac{Q}{B}\Gamma(\alpha+2)\,\xi^q + \cdots \right\}, \tag{4.10}
$$

where

$$
r = \alpha - p + q(\alpha+1) + 1, \qquad Q = \frac{\alpha(1+q)/2 + q - p + 1}{q}. \tag{4.11}
$$

Making use of (4.8) and (4.10), dominant balance as $\xi \to 0$ in Eq. (4.1) requires

$$
(2-\xi)\,\xi^{1-p} \sim \frac{2A}{(qB)^{\alpha+1}} \xi^r \left\{ \Gamma(\alpha+1) + \frac{A\,c\,\Gamma(2\alpha+2)}{(qB)^{\alpha+1}} \xi^{(\alpha+1)(1+q)} \right.
$$
$$
\left. + \frac{Q}{B}\Gamma(\alpha+2)\,\xi^q + \cdots \right\}. \tag{4.12}
$$

To leading order, this is achieved if

$$
r = 1 - p, \quad (qB)^{\alpha+1} = A\Gamma(\alpha+1). \tag{4.13}
$$

Using (4.11), the first of these conditions specifies

$$
q = -\frac{\alpha}{\alpha+1}, \tag{4.14}
$$

with $q > 0$ for $-1 < \alpha < 0$, as assumed in (4.8). The second condition in (4.13) then determines $B > 0$, as long as $A > 0$; if $A < 0$, the ansatz (4.8) is not appropriate (see also Section 4.4 below).

Assuming $A > 0$, now we examine the balance of next-order terms in (4.12) in hopes of determing the power p in (4.8). In view of (4.14), ($\alpha +$

$1)(1 + q) = 1$, so for $0 < q < 1$ (i.e. $-1/2 < \alpha < 0$) the $O(\xi^{r+q})$ term dominates and it cannot be balanced unless $Q = 0$, which according to (4.11), implies

$$p = 1 + \frac{q}{2} \quad \left(-\frac{1}{2} < \alpha < 0 \right). \tag{4.15}$$

For $\alpha = -1/2$ ($q = 1$), the three next-order terms in (4.12) are $O(\xi^{r+1})$. From this balance, making use of (2.3), (4.11), (4.13) and (4.14), we find

$$p = \frac{3}{2} + 3\pi A^2 \quad \left(\alpha = -\frac{1}{2} \right). \tag{4.16}$$

When $\alpha < -1/2$ ($q > 1$), however, the $O(\xi^{r+q})$ term in (4.12) is subdominant and no balance is possible at $O(\xi^{r+1})$. This difficulty is handled by modifying the exponential in Eq. (4.8),

$$\exp\left(\frac{B}{\xi^q} \right) \to \exp\left\{ \frac{B}{\xi^q}(1 + b\xi) \right\}, \tag{4.17}$$

where b is a constant. It should be noted that, when $\alpha < -1/2$ ($q > 1$), $\exp\left(Bb\,\xi^{1-q} \right)$ may not be expanded in powers of ξ. By choosing b suitably, it is now possible to balance $O(\xi^{r+1})$ terms in (4.12). Furthermore, the $O(\xi^{r+q})$ term is removed by setting $Q = 0$, so the expression (4.15) for p still holds. Details will not be pursued here.

4.4. The limit $|A| \ll 1$

It is worth noting that the singularity in Eq. (4.8) does not reduce to a simple pole in the linear limit ($A = 0$). This suggests that, for $-1 < \alpha < 0$, the nonlinear term of the outer equation (4.1) acts as a singular perturbation when $|A| \ll 1$ and $\kappa \approx 1$. Indeed, expanding U in powers of A

$$U(\kappa; A) = U_0(\kappa) + AU_1(\kappa) + \cdots, \tag{4.18}$$

14

we find from Eq. (4.1), in the limit $\xi \equiv 1 - \kappa \to 0$,

$$U_0 = \frac{\kappa^\alpha}{1 - \kappa^2} \sim \frac{1}{2\,\xi}, \tag{4.19}$$

$$U_1 = \frac{2}{1 - \kappa^2} \int_0^{\kappa/2} U_0(\lambda) U_0(\kappa - \lambda) \mathrm{d}\lambda \sim \frac{\pi}{2} \frac{\xi^{\alpha-1}}{\sin(\alpha+1)\pi}. \tag{4.20}$$

As expected, expansion (4.18) becomes disordered as $\xi \to 0$ and a separate expansion in terms of re-scaled variables is needed in the vicinity of $\kappa = 1$. This boundary-layer-type analysis provides independent confirmation of the ansatz (4.8) along with an asymptotic expression for the constant C_- for $0 < A \ll 1$. Furthermore, from this analysis we deduce the behavior of $U(\kappa)$ as $\kappa \to 1$ in the case $A < 0$, where (4.8) is not appropriate. Here, we briefly outline the main results.

The disordering of expansion (4.18) suggests the following re-scaled variables when $\kappa \approx 1$

$$U(\kappa) = |A|^{1/\alpha}\, \tilde{U}(\tilde{\xi}), \qquad \tilde{\xi} = |A|^{1/\alpha}(1 - \kappa). \tag{4.21}$$

Substituting (4.21) in Eq. (4.3) leads to the following integral equation for $\tilde{U}(\tilde{\xi})$

$$\tilde{\xi}\tilde{U}'(\tilde{\xi}) + \tilde{U}(\tilde{\xi}) - \mathrm{sgn}A \int_0^\infty \lambda^\alpha \tilde{U}'(\tilde{\xi} + \lambda)\mathrm{d}\lambda = 0, \tag{4.22}$$

where prime indicates derivative with respect to $\tilde{\xi}$ and $\mathrm{sgn}A = \pm 1$ ($A \gtrless 0$). This equation is to be solved subject to the matching condition

$$\tilde{U}(\tilde{\xi}) \sim \frac{1}{2\,\tilde{\xi}} \qquad (\tilde{\xi} \gg 1), \tag{4.23}$$

in keeping with (4.19). The solution is found by transforms and can be expressed as

$$\tilde{U}(\tilde{\xi}) = \frac{1}{2} \int_0^\infty \mathrm{d}s \exp\left\{ -\tilde{\xi}s - \mathrm{sgn}A \frac{\Gamma(\alpha)}{s^\alpha} \right\}. \tag{4.24}$$

15

To examine the behavior of $U(\kappa)$ as $\kappa \to 1$, we evaluate the integral in Eq. (4.24) asympotically for $\tilde{\xi} \to 0$ using Laplace's method [12]. As expected, the result hinges on $\mathrm{sgn}A = \pm 1$. Specifically, for $A > 0$, we find

$$\tilde{U}(\tilde{\xi}) \sim \sqrt{\frac{\pi}{2(\alpha+1)}} \frac{(\Gamma(\alpha+1))^{\frac{1}{2(\alpha+1)}}}{\tilde{\xi}^p} \exp\left\{\frac{BA^{-\frac{1}{\alpha+1}}}{\tilde{\xi}^q}\right\} \quad (\tilde{\xi} \to 0), \quad (4.25)$$

where q, B and p are given by Eqs. (4.13)–(4.15). In view of (4.21), this result is in agreement with Eq. (4.8) and

$$C_- \sim \sqrt{\frac{\pi}{2(\alpha+1)}} (A\Gamma(\alpha+1))^{\frac{1}{2(\alpha+1)}} \quad (0 < A \ll 1). \quad (4.26)$$

On the other hand, for $A < 0$, $\tilde{U}(\tilde{\xi})$ approaches a constant as $\tilde{\xi} \to 0$,

$$\tilde{U}(\tilde{\xi}) \sim -\frac{1}{2\alpha} \Gamma\left(-1/\alpha\right)\left(-\Gamma(\alpha)\right)^{\frac{1}{\alpha}} \quad (\tilde{\xi} \to 0). \quad (4.27)$$

The asymptotic results (4.25)–(4.27) are consistent with numerical solutions of Eq. (4.1) (see Section 7.2).

5. Wave response for $\alpha > 0$

As noted in Section 4.1, for $\alpha > 0$, the residues of the poles of $\hat{u}(k)$ at $k = \pm 1/\mu$ are determined from the outer equation alone. Specifically, combining (4.4) with (3.1) and using $\hat{u}(-k) = \hat{u}(k)^*$, we find

$$\hat{u}(k) \sim \mp \frac{AC}{\mu^{\alpha+1}} \frac{\mathrm{e}^{-\beta/\mu}}{k \mp 1/\mu} \quad (k \to \pm 1/\mu). \quad (5.1)$$

Then, inverting the Fourier transform,

$$u(x) = \int_{\mathscr{L}} \hat{u}(k)\,\mathrm{e}^{\mathrm{i}kx}\mathrm{d}k, \quad (5.2)$$

where the integration path $\mathscr{L}$ extends along the real k-axis but passes below $k = \pm 1/\mu$ so as to observe the radiation condition (1.2), the residues in

16

Eq. (5.1) contribute a radiating wave downstream in the form of Eq. (1.3) with

$$R = 4\pi AC \frac{e^{-\beta/\mu}}{\mu^{\alpha+1}}, \qquad \theta = -\frac{\pi}{2}. \qquad (5.3)$$

According to Eq. (5.3), nonlinearity affects the wave amplitude R but not the phase shift θ, and the only difference of the nonlinear from the linear wave response

$$R_{\mathrm{lin}} = 2\pi A \frac{e^{-\beta/\mu}}{\mu^{\alpha+1}}, \qquad \theta_{\mathrm{lin}} = -\frac{\pi}{2}, \qquad (5.4)$$

is the value of C, which depends on A and α. By contrast, in the linear solution above $C = 1/2$ irrespective of α. We have computed $C(A, \alpha)$ numerically by integrating Eq. (4.1) as an initial-value problem, using (4.2) as initial condition and marching towards the simple pole of $U(\kappa)$ at $\kappa = 1$ according to Eq. (4.4). Figure 1 plots $|R/R_{\mathrm{lin}}| = 2|C|$, the ratio of the non-linear to the linear response amplitude, as a function of $-3 \leq A \leq 3$ for $\alpha = 0.5$, 1 and 2. Nonlinearity becomes more important as α is decreased, and the validity of the linear theory is rather limited when $\alpha \lesssim 1$. Furthermore, in this range of α, the polarity of the forcing is a significant factor, as the nonlinear response amplitude is greatly enhanced (reduced) for $A > 0$ ($A < 0$).

Theoretically, for $\alpha > 0$, the nonlinear wave response is determined solely by the behavior of $\hat{f}(k)$ for large k (viz., Eq. (1.7)), regardless of the details of the forcing profile $f(x)$. We have tested this theoretical prediction by numerically computing directly from the fKdV equation (1.1) nonlinear

wave responses to three different $f(x)$ whose Fourier transforms

$$\text{(i) } \hat{f}(k) = \frac{A}{2} \left(\frac{k}{\tanh(\pi k/2)} \right)^{\alpha} \text{sech} \frac{\pi k}{2},$$

$$\text{(ii) } \hat{f}(k) = A \left(\frac{k}{\tanh(\pi k/2)} \right)^{\alpha} \exp \left(-\frac{\pi |k|}{2} \right), \qquad (5.5)$$

$$\text{(iii) } \hat{f}(k) = \frac{A}{2} \frac{k^4}{k^4 + 1} \left(\frac{k}{\tanh(\pi k/2)} \right)^{\alpha} \text{sech} \frac{\pi k}{2},$$

obey the asymptotic behavior in Eq. (1.7). (The fKdV equation was integrated numerically by a standard fourth-order Runge–Kutta finite-difference method with $\Delta x = 0.02$, starting from far upstream where $u \rightarrow 0$ and marching toward downstream.) These computations were carried out for the same α as above and two values of the small parameter $\mu = 0.1,\ 0.2$ with $\varepsilon = \mu^{\alpha+1}$ according to Eq. (2.6). The numerical results for the ratio of the nonlinear to the linear wave amplitude are compared with the theoretical plots in Fig. 1. For (i) and (ii), the direct numerical computations with $\mu = 0.2$ are in good agreement with the theory while for (iii) it is necessary to reduce μ to 0.1 to achieve fair agreement. This difference is attributed to the fact that (iii) approaches the assumed behavior in Eq. (1.7) at larger k than (i) and (ii).

The fair agreement between the asymptotic and numerical results in Fig. 1 for the forcing profile (iii) can be greatly improved (see Fig. 2) by taking into account, via an inner solution, the effect of the second integral in Eq. (3.7), which formally is subdominant for $\alpha > 0$. This higher-order analysis is outlined in the Appendix.

6. Wave response for $\alpha = 0$

As noted in Section 4.2, for $\alpha = 0$, the outer equation (4.1) breaks down in the vicinity of $\kappa = 1$. Thus, we now return to Eq. (3.7) and seek a local
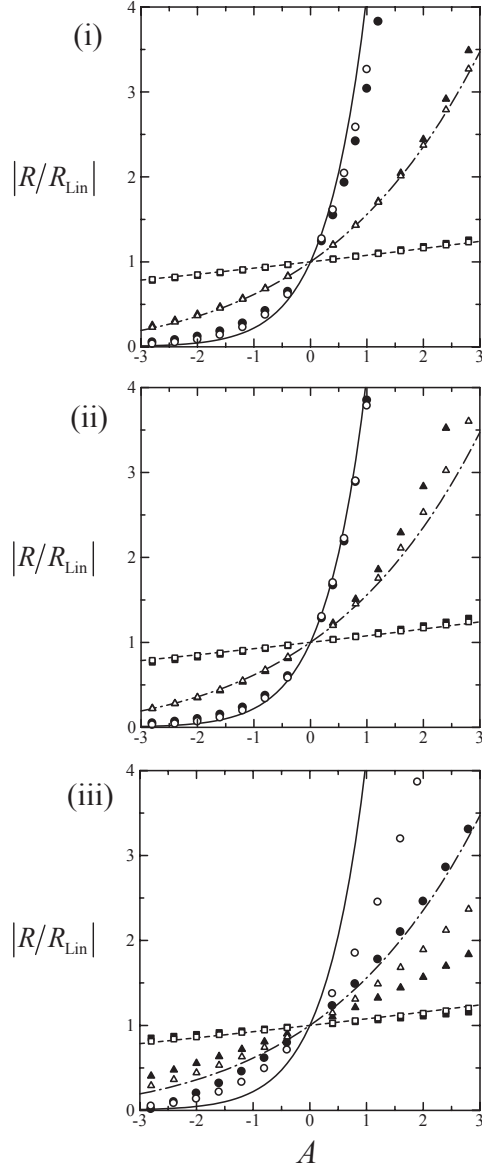
Figure 1: Ratio of nonlinear to linear wave amplitude as a function of the forcing amplitude A for $\alpha = 0.5$ (solid line), 1 (dash-dot line) and 2 (dashed line). The shapes (circles: $\alpha = 0.5$, triangles: $\alpha = 1$, squares: $\alpha = 2$) correspond to numerical results from direct integration of Eq. (1.1), subject to the forcing terms (i), (ii) and (iii) specified in Eq. (5.5), for $\mu = 0.1$ (open shapes), $\mu = 0.2$ (filled shapes) and $\varepsilon = \mu^{\alpha+1}$.
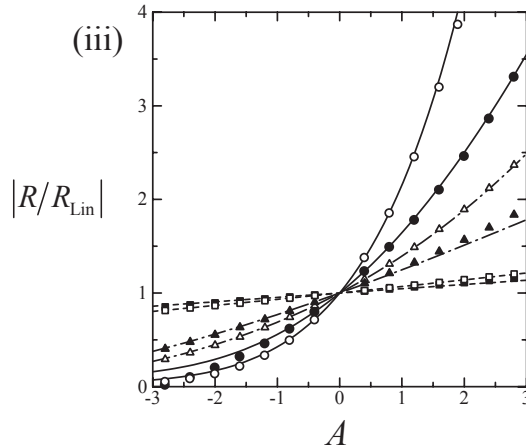
19

Figure 2: Ratio of nonlinear to linear wave amplitude, based on the higher-order analysis outlined in the Appendix, as a function of the forcing amplitude A for the forcing term (iii) specified in Eq. (5.5) with $\alpha = 0.5$ (solid lines), 1 (dash-dot lines) and 2 (dashed lines). The shapes (circles: $\alpha = 0.5$, triangles: $\alpha = 1$, squares: $\alpha = 2$) correspond to numerical results for $\mu = 0.1$ (open shapes), $\mu = 0.2$ (filled shapes) and $\varepsilon = \mu^{\alpha+1}$.

solution that reveals the simple pole of $U(\kappa)$ at $\kappa = 1$. This 'inner' analysis is sketched below, followed by a discussion of the nonlinear wave response.

6.1. Inner analysis

Consider first $A > -1$. Upon differentiating Eq. (3.7),

$$(1 - \kappa^2)U'(\kappa) - 2\kappa U(\kappa) - AU(\kappa/2)^2$$

$$- 2A \int_{\mu/\delta}^{\kappa/2} U(\lambda)U'(\kappa - \lambda)\mathrm{d}\lambda - 2\mu \int_{-\infty}^{1/\delta} \hat{f}(l)U'(\kappa - \mu l)\,\mathrm{e}^{\beta l}\mathrm{d}l \qquad (6.1)$$

$$= 0,$$

the singular behavior of the outer solution as $\kappa \to 1$ (viz., Eq. (4.5)) suggests that the second integral term in Eq. (6.1), which was neglected in the outer analysis, partakes in the dominant balance when $\kappa = 1 + O(\mu)$. This

20

motivates the re-scaling

$$U(\kappa) = \frac{\tilde{U}(\tilde{\kappa})}{\mu^{1+A}}, \qquad \tilde{\kappa} = \frac{1-\kappa}{\mu}. \tag{6.2}$$

In terms of these variables, Eq. (6.1) is approximated correct to $O(1/\mu^{1+A})$ by the inner equation

$$\tilde{\kappa}\tilde{U}'(\tilde{\kappa}) + \tilde{U}(\tilde{\kappa}) - \int_{-\infty}^{\infty} \hat{f}(l)\tilde{U}'(\tilde{\kappa}-l)\,\mathrm{e}^{-\beta l}\mathrm{d}l = 0, \tag{6.3}$$

where prime indicates derivative with respect to $\tilde{\kappa}$.

Following [7, 11], Eq. (6.3) is solved by the one-sided Fourier transform

$$\tilde{U}(\tilde{\kappa}) = \int_0^{\infty} \Phi(s)\mathrm{e}^{\mathrm{i}s\tilde{\kappa}}\mathrm{d}s. \tag{6.4}$$

The integral above converges when $\operatorname{Im}\tilde{\kappa} > 0$ so $\operatorname{Im}\kappa < 0$ according to (6.2), in keeping with the radiation condition (1.2) which requires the integration path $\mathscr{L}$ in inverting $\hat{u}(k)$ (viz., Eq. (5.2)) to pass below the poles at $k = \pm 1/\mu$. Substituting Eq. (6.4) in Eq. (6.3) and assuming $s\Phi(s) \to 0$ as $s \to 0$ (verified below), $\Phi(s)$ satisfies

$$\frac{\mathrm{d}\Phi}{\mathrm{d}s} + \mathrm{i}f(s - \mathrm{i}\beta)\,\Phi = 0. \tag{6.5}$$

Therefore,

$$\Phi = \tilde{C}_1 \exp\left\{\mathrm{i}\int_s^{\infty} f(s' - \mathrm{i}\beta)\mathrm{d}s'\right\}, \tag{6.6}$$

where $\tilde{C}_1$ is a constant that will be specified by matching with the outer solution. It should be noted that in view of Eq. (1.7) $\mathrm{i}f(s-\mathrm{i}\beta) \sim -A/s$ ($s \to 0$) so $\Phi = O(s^A)$ and $s\Phi(s) \to 0$, as assumed above. Then, inserting Eq. (6.6) in Eq. (6.4) yields the inner solution

$$\tilde{U}(\tilde{\kappa}) = \tilde{C}_1 \int_0^{\infty} \exp\left\{\mathrm{i}\left(s\tilde{\kappa} + \int_s^{\infty} f(s' - \mathrm{i}\beta)\mathrm{d}s'\right)\right\}\mathrm{d}s. \tag{6.7}$$

21

From Eq. (6.7) we find that

$$\tilde{U}(\tilde{\kappa}) \sim \mathrm{i}\,\frac{\tilde{C}_1}{\tilde{\kappa}} \quad (\tilde{\kappa} \to 0). \tag{6.8}$$

In view of Eq. (6.2), this confirms that $U(\kappa)$ features a simple pole at $\kappa = 1$

$$U(\kappa) \sim \mathrm{i}\,\frac{\tilde{C}_1}{\mu^A}\,\frac{1}{1-\kappa} \quad (\kappa \to 1). \tag{6.9}$$

To determine $\tilde{C}_1$, we examine the outer limit ($\tilde{\kappa} \gg 1$) of the inner solution. Returning to Eq. (6.7), the integral is evaluated asymptotically for $\tilde{\kappa} \gg 1$ by first approximating the integrand in the neighborhood of $s = 0$ using

$$\mathrm{i}\int_s^\infty f(s' - \mathrm{i}\beta)\mathrm{d}s' \sim A\ln s + J + \cdots \quad (s \to 0), \tag{6.10}$$

where J is the (generally complex) constant

$$J = \int_0^1 \left\{ \mathrm{i}f(s' - \mathrm{i}\beta) + \frac{A}{s'} \right\}\mathrm{d}s' + \int_1^\infty \mathrm{i}f(s' - \mathrm{i}\beta)\mathrm{d}s', \tag{6.11}$$

and then rotating the integration path to the positive imaginary s-axis. Thus, we find

$$\tilde{U}(\tilde{\kappa}) \sim \mathrm{i}^{1+A}\,\mathrm{e}^J\,\Gamma(1+A)\frac{\tilde{C}_1}{\tilde{\kappa}^{1+A}} \quad (\tilde{\kappa} \gg 1). \tag{6.12}$$

This expression matches with the inner limit ($\kappa \to 1$) of the outer solution (viz., Eq. (4.5)) if

$$\tilde{C}_1 = \frac{\mathrm{e}^{-J}C_1}{\mathrm{i}^{1+A}\Gamma(2+A)}. \tag{6.13}$$

The above inner analysis can be readily adapted to $A \leq -1$. Briefly, suppose $-n < A \leq -n+1$, where $n \geq 2$ is integer. Motivated by the singular behavior as $\kappa \to 1$ of the outer solution (viz., Eq. (4.7)), the appropriate rescaling is

$$U^{(n-1)}(\kappa) = \frac{\tilde{U}(\tilde{\kappa})}{\mu^{n+A}}, \tag{6.14}$$

22

with $\tilde\kappa$ still given by Eq. (6.2).Then, differentiating Eq. (6.1) $n-1$ times and substituting Eq. (6.14), the inner equation (6.3) is replaced by

$$\tilde\kappa \tilde{U}' + n\tilde{U}(\tilde\kappa) - \int_{-\infty}^{\infty} \hat{f}(l)\tilde{U}'(\tilde\kappa - l)\, \mathrm{e}^{-\beta l}\mathrm{d}l = 0. \qquad (6.15)$$

The inner solution again is posed in the form of Eq. (6.4), which upon substitution in Eq. (6.15) implies

$$s\frac{\mathrm{d}\Phi}{\mathrm{d}s} - (n-1)\Phi + \mathrm{i}sf(s - \mathrm{i}\beta)\,\Phi = 0. \qquad (6.16)$$

Therefore,

$$\Phi(s) = \tilde{C}_n s^{n-1} \exp\left\{\mathrm{i}\int_s^{\infty} f(s' - \mathrm{i}\beta)\mathrm{d}s'\right\} \qquad (6.17)$$

so the inner solution reads

$$\tilde{U}(\tilde\kappa) = \tilde{C}_n \int_0^{\infty} s^{n-1} \exp\left\{\mathrm{i}\left(s\tilde\kappa + \int_s^{\infty} f(s' - \mathrm{i}\beta)\mathrm{d}s'\right)\right\}\mathrm{d}s, \qquad (6.18)$$

where $\tilde{C}_n$ is a constant.

Now, in the limit $\tilde\kappa \to 0$, Eq. (6.18) yields

$$\tilde{U}(\tilde\kappa) \sim \mathrm{i}^n(n-1)!\,\frac{\tilde{C}_n}{\tilde\kappa^n}, \qquad (6.19)$$

which, in view of (6.14), translates into

$$U^{(n-1)}(\kappa) \sim \mathrm{i}^n\frac{\tilde{C}_n}{\mu^A}\frac{(n-1)!}{(1-\kappa)^n} \quad (\kappa \to 1). \qquad (6.20)$$

Hence, $U(\kappa)$ features a simple pole at $\kappa = 1$,

$$U(\kappa) \sim \mathrm{i}^n\frac{\tilde{C}_n}{\mu^A}\frac{1}{1-\kappa} \quad (\kappa \to 1). \qquad (6.21)$$

The constant $\tilde{C}_n$ is determined by matching the outer limit ($\tilde\kappa \gg 1$) of the inner solution (6.18),

$$\tilde{U}(\tilde\kappa) \sim \mathrm{i}^{n+A}\, \mathrm{e}^J\, \Gamma(n+A)\frac{\tilde{C}_n}{\tilde\kappa^{n+A}} \quad (\tilde\kappa \gg 1), \qquad (6.22)$$

23

with the inner limit ($\kappa \to 1$) of the outer solution (viz., Eq. (4.7)). Thus, we find

$$\tilde{C}_n = \frac{\mathrm{e}^{-J}C_n}{\mathrm{i}^{n+A}\,\Gamma(n+1+A)}. \tag{6.23}$$

Finally, Eqs. (6.9) and (6.13) can be combined with Eqs. (6.21) and (6.23) to a single expression, valid both when $A > -1$ ($n = 1$) and $-n < A \le -n+1$ ($n \ge 2$), for the simple pole of $U(\kappa)$ at $\kappa = 1$,

$$U(\kappa) \sim \frac{1}{(\mathrm{i}\mu)^A}\,\frac{\mathrm{e}^{-J}C_n}{\Gamma(n+1+A)}\,\frac{1}{1-\kappa} \quad (\kappa \to 1). \tag{6.24}$$

6.2. Radiating waves

By combining Eq. (6.24) with Eq. (3.1) and making use of $\hat{u}(-k) = \hat{u}^*(k)$, we obtain the following expression for the simple poles of $\hat{u}(k)$ at $k = \pm 1/\mu$

$$\hat{u}(k) \sim \mp\frac{AC_n\exp(-J_r \mp \mathrm{i}J_i)}{(\pm\mathrm{i})^A\,\Gamma(n+1+A)}\,\frac{\mathrm{e}^{-\beta/\mu}}{\mu^{1+A}}\,\frac{1}{k \mp 1/\mu} \quad (k \to \pm 1/\mu), \tag{6.25}$$

where $J = J_r + \mathrm{i}J_i$ was defined in Eq. (6.11). Inverting the Fourier transform $\hat{u}(k)$ as in Eq. (5.2), the residues of these poles give rise to a wavetrain downstream in the form of Eq. (1.3), whose amplitude R and phase shift θ are given by

$$R = \frac{4\pi A\,C_n\,\mathrm{e}^{-J_r}}{\Gamma(n+1+A)}\,\frac{\mathrm{e}^{-\beta/\mu}}{\mu^{1+A}}, \qquad \theta = -(1+A)\frac{\pi}{2} - J_i. \tag{6.26}$$

Here, in keeping with Eq. (6.24), the positive integer n is specified by the forcing amplitude A: $n = 1$ for $A > -1$ and $n \ge 2$ for $-n < A \le -n+1$.

It should be noted that for the forcing profile $f(x) = A\operatorname{sech} x$ (corresponding to (i) in Eq. (5.5) with $\alpha = 0$), $\mathrm{e}^{-J} = 2^A$ according to Eq. (6.11). Thus, the final results in Eq. (6.26) agree with those found earlier for this forcing in the cases $A = 1$ [7] and $A = \sigma\varepsilon^{-1/2}$ ($\sigma > 0$) [11].

Compared with the wave response for $\alpha > 0$ (viz., Eq. (5.3)), here nonlinear effects are more pronounced. Specifically, the power of μ in Eq. (6.26)

24

for the wave amplitude R is controlled by the forcing amplitude A, so for $A > 0$ (< 0) the order of magnitude of R is larger (smaller) than the linear response (viz., Eq. (5.4)). In addition, nonlinearity affects R through the dependence on A of the constants C_n, e^{-J_r} and $\Gamma(n + 1 + A)$, which in the linear limit $(A = 0,\ n = 1)$ take the values $1/2$, 1 and 1, respectively. Furthermore, the phase shift θ in Eq. (6.26) depends on A explicitly and through J_i $(= 0$ in the linear limit). It should be noted that $J = J_r + \mathrm{i}J_i$ (viz., Eq. (6.11)) depends on the specific forcing profile $f(x)$, not just the asymptotic behavior of $\hat{f}(k)$ for $|k| \gg 1$; hence, the nonlinear wave response does so as well.

To illustrate the effects of nonlinearity for $\alpha = 0$, Fig. 3 shows plots of $|R/R_{\mathrm{lin}}|$, the ratio of the nonlinear to the linear response amplitude, as a function of $-3 \leq A \leq 3$ for the forcing profiles (i)–(iii) in Eq. (5.5) (with $\alpha = 0$) and for the values of $\mu = 0.2$ and 0.5. As in Section 5, the constants C_n in Eq. (6.26) were computed numerically from the outer equation (4.1) by marching forward in κ and fitting the asymptotic behavior as $\kappa \to 1$ predicted by dominant balance (viz., Eqs. (4.5), (4.7)). In addition, Fig. 3 shows results from direct numerical solution of the fKdV equation (1.1) for the same three forcings $f(x)$ and two values of μ (with $\varepsilon = \mu$) as above. Similar to the case $\alpha > 0$ (Fig. 1), for the forcing profiles (i) and (ii) the theoretical predictions agree well with the numerical results for both values of μ, while for (iii) there is reasonable agreement for the smaller $\mu = 0.2$ only.

It is worth noting the steep increase (decrease) of the wave amplitude caused by nonlinearity when $A > 0$ $(A < 0)$. This striking nonlinear feature is further illustrated in Fig. 4, which shows theoretical plots and numerical results of the absolute value $|R|$ of the wave amplitude as a function of
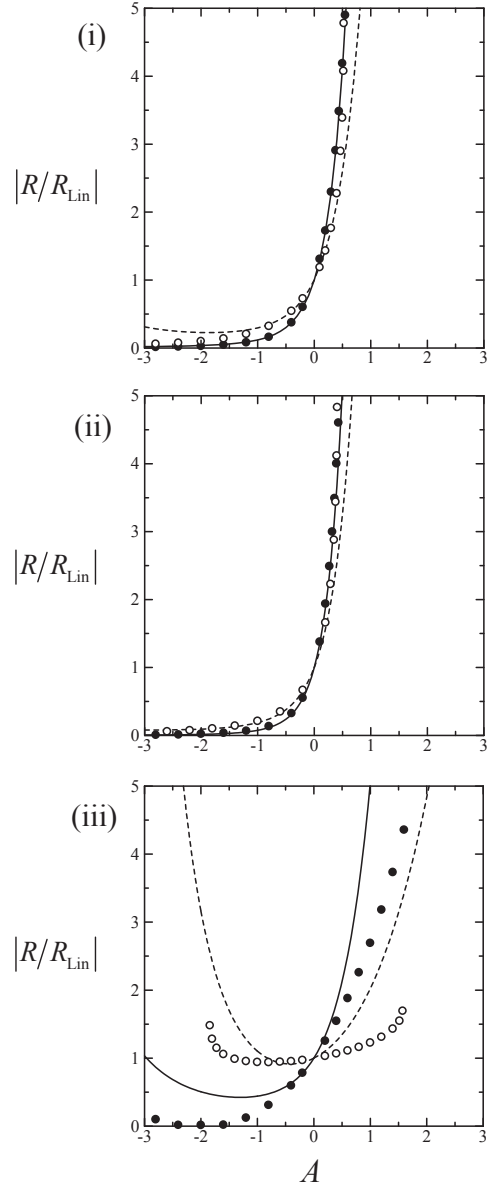
25

Figure 3: Ratio of nonlinear to linear wave amplitude as a function of the forcing amplitude A for $\alpha = 0$ with $\mu = 0.2$ (solid line) and 0.5 (dashed line), corresponding to the forcing terms (i), (ii) and (iii) specified in Eq. (5.5). The circles (filled: $\mu = 0.2$, open: $\mu = 0.5$) are numerical results from direct integration of Eq. (1.1) subject to these forcing terms and $\varepsilon = \mu$.
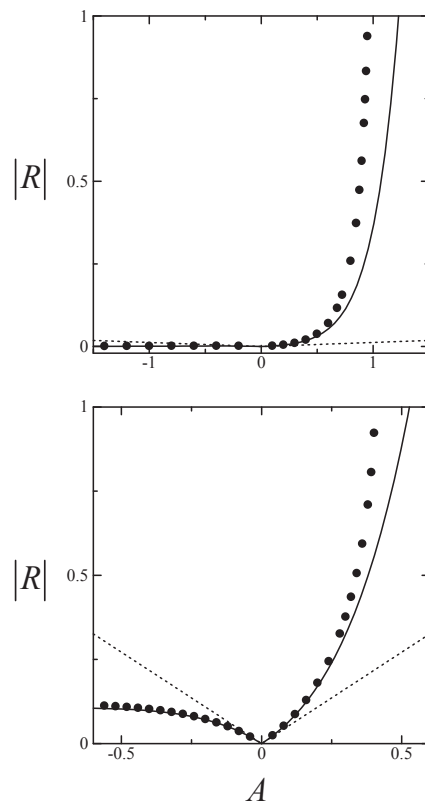
Figure 4: Wave amplitude $|R|$ as a function of A for the forcing $f(x) = A\pi/(x^2 + \pi^2/4)$ with $\mu = 0.2$ (top) and 0.5 (bottom). The solid and dotted lines are nonlinear and linear responses, respectively. The circles denote numerical results from direct integration of Eq. (1.1) subject to this forcing term and $\varepsilon = \mu$.
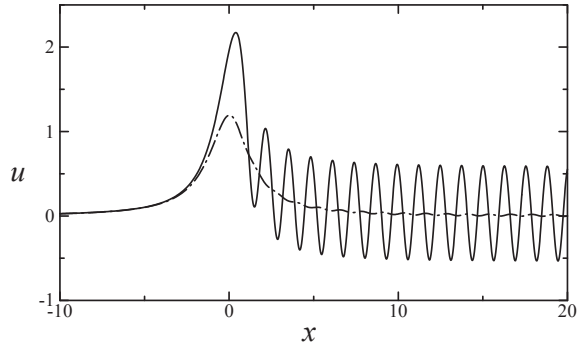
Figure 5: Computed profile $u(x)$ of the fKdV equation (1.1) subject to the forcing $f(x) = A\pi/(x^2 + \pi^2/4)$ with $\varepsilon = \mu = 0.2$ and $A = 0.9$ ($\varepsilon A = 0.18$). The solid and dash-dot lines are nonlinear and linear solutions, respectively.

the forcing amplitude A, for the algebraic forcing $f(x) = A\pi/(x^2 + \pi^2/4)$ (corresponding to (ii) in Eq. (5.5) with $\alpha = 0$) and the values of $\mu = 0.2$, 0.5. Compared with the linear solution (viz., Eq. (5.4)), which is limited to $|A| \ll 1$, the exponential asymptotics theory has a much broader range of validity in terms of A; moreover, it captures the nonlinear wave response for even moderate values of μ, when the (formally exponentially small in μ) $|R|$ is comparable to A. In such a case, the radiating waves can form the dominant part of the response, as illustrated in Fig. 5 for $\mu = 0.2$ and $A = 0.9$.

7. Wave response for $-1 < \alpha < 0$

For $-1 < \alpha < 0$, again the outer solution breaks down when $\kappa = 1 + O(\mu)$ so an inner analyis is required to reveal the simple pole of $U(\kappa)$ at $\kappa = 1$. Similar to the outer analysis (Section 4.3), the sign of A is an important factor in the inner analysis. Here, in the interest of brevity, we shall focus on the case $A > 0$, for which nonlinear effects turn out to be

28

most dramatic. Furthermore, only the leading-order inner solution, which ignores the corrections to the exponential singularity of the outer solution (viz., Eq. (4.17)) that arise when $\alpha < -1/2$, will be considered.

7.1. Inner analysis

The behavior of the outer solution as $\kappa \to 1$ (viz., Eq. (4.8)) suggests the following inner variables

$$U(\kappa) = \frac{\tilde{U}(\tilde{\kappa})}{\mu^p}, \quad \tilde{\kappa} = \frac{1 - \kappa}{\mu}, \tag{7.1}$$

where $p = 1 + q/2 = (\alpha + 2)/2(\alpha + 1)$ according to Eqs. (4.14)–(4.15). Substituting Eq. (7.1) into Eq. (3.7) then leads to

$$\tilde{\kappa}\tilde{U}(\tilde{\kappa}) - \mu^\alpha \int_{-\infty}^{\infty} \hat{f}(l)\tilde{U}(\tilde{\kappa} - l)\mathrm{e}^{-\beta l}\mathrm{d}l = 0. \tag{7.2}$$

Unlike the case $\alpha = 0$, here the inner equation involves the small parameter μ explicitly, which may be attributed to the exponential rather than algebraic singularity of the outer solution at $\kappa = 1$.

The inner solution again is posed in the form (6.4), where $\Phi(s)$ satisfies

$$\frac{\mathrm{d}\Phi}{\mathrm{d}s} + \mathrm{i}\mu^\alpha f(s - \mathrm{i}\beta)\Phi = 0, \tag{7.3}$$

on the assumption that $\Phi(0)$ can be dropped (justified below). Thus,

$$\Phi(s) = \tilde{C}_- \exp\left\{\mathrm{i}\mu^\alpha \int_s^\infty f(s' - \mathrm{i}\beta)\mathrm{d}s'\right\}, \tag{7.4}$$

where $\tilde{C}_-$ is a constant. It should be noted that, in view of Eq. (1.7),

$$f(s - \mathrm{i}\beta) \sim \left(\frac{\mathrm{i}}{s}\right)^{\alpha+1} A\Gamma(\alpha + 1) \quad (s \to 0), \tag{7.5}$$

so $\Phi(0)$ is finite. However, as argued below, $|\Phi(0)| \ll |\tilde{\kappa}\tilde{U}(\tilde{\kappa})|$, which justifies dropping $\Phi(0)$ in deducing Eq. (7.3) from Eq. (7.2).

Inserting Eq. (7.4) in Eq. (6.4) yields the inner solution

$$\tilde{U}(\tilde{\kappa}) = \tilde{C}_- \int_0^\infty \exp\left\{ i\left(s\tilde{\kappa} + \mu^\alpha \int_s^\infty f(s' - i\beta)ds' \right) \right\} ds, \qquad (7.6)$$

from which it follows that

$$\tilde{U}(\tilde{\kappa}) \sim i\frac{\tilde{C}_-}{\tilde{\kappa}} \quad (\tilde{\kappa} \to 0). \qquad (7.7)$$

In view of Eq. (7.1), this confirms that $U(\kappa)$ features a simple pole at $\kappa = 1$

$$U(\kappa) \sim \frac{i}{\mu^{q/2}} \frac{\tilde{C}_-}{1 - \kappa} \quad (\kappa \to 1). \qquad (7.8)$$

The constant $\tilde{C}_-$ is determined by inner–outer solution matching. To this end, making use of Eq. (7.5) we expand the exponent in the inner solution (7.6)

$$i \int_s^\infty f(s' - i\beta)ds' \sim J_- - A\Gamma(\alpha) \left(\frac{i}{s} \right)^\alpha + \cdots \quad (s \to 0), \qquad (7.9)$$

where J_- is the (generally complex) constant

$$J_- = i \int_0^\infty f(s' - i\beta)ds'. \qquad (7.10)$$

The integral in Eq. (7.6) then is evaluated asymptotically for $\mu^\alpha \ll \tilde{\kappa} \ll \mu^{-1}$ by substituting Eq. (7.9) and rotating the integration path to the positive imaginary s-axis via $s = i\,(\mu^\alpha/\tilde{\kappa})^{1/(\alpha+1)}\,y$

$$\tilde{U}(\tilde{\kappa}) \sim i\mu\tilde{C}_- \frac{e^{\mu^\alpha J_-}}{(\mu\tilde{\kappa})^{q+1}} \int_0^\infty \exp\left\{ -\frac{1}{(\mu\tilde{\kappa})^q} \left(y + \frac{A\Gamma(\alpha)}{y^\alpha} \right) \right\} dy. \qquad (7.11)$$

Since $1/(\mu\tilde{\kappa})^q \gg 1$, by Laplace's method [12], the main contribution to the integral above comes from the neighborhood of $y = (A\Gamma(\alpha + 1))^{1/(\alpha+1)}$ where the exponent attains its maximum. Thus, we find

$$\tilde{U}(\tilde{\kappa}) \sim i\mu\tilde{C}_- \frac{e^{\mu^\alpha J_-}}{(\mu\tilde{\kappa})^p} \sqrt{\frac{2\pi}{\alpha + 1}} \, (A\Gamma(\alpha + 1))^{\frac{1}{2(\alpha+1)}} \exp\left\{ \frac{B}{(\mu\tilde{\kappa})^q} \right\} \quad (\tilde{\kappa} \gg 1), \qquad (7.12)$$

where q, B and p are given by Eqs. (4.13)–(4.15). Taking into account Eq. (7.1), this outer limit of the inner solution matches with the inner limit of the outer solution (viz., Eq. (4.8)) if

$$\tilde{C}_- = -\mathrm{i}\mu^{q/2}\frac{C_-\,\mathrm{e}^{-\mu^\alpha J_-}}{(A\Gamma(\alpha+1))^{\frac{1}{2(\alpha+1)}}}\sqrt{\frac{\alpha+1}{2\pi}}. \tag{7.13}$$

Accordingly, Eq. (7.8) for the simple pole of $U(\kappa)$ at $\kappa = 1$ reads

$$U(\kappa) \sim \frac{C_-\,\mathrm{e}^{-\mu^\alpha J_-}}{(A\Gamma(\alpha+1))^{\frac{1}{2(\alpha+1)}}}\sqrt{\frac{\alpha+1}{2\pi}}\frac{1}{1-\kappa} \quad (\kappa \to 1). \tag{7.14}$$

Finally, we verify that $|\Phi(0)| \ll |\tilde{\kappa}\tilde{U}(\tilde{\kappa})|$. From Eqs. (7.4) and (7.6), it follows that

$$\frac{\tilde{\kappa}\tilde{U}(\tilde{\kappa})}{\Phi(0)} = \int_0^\infty \exp\left\{\mathrm{i}\left(z - \mu^\alpha \int_0^{z/\tilde{\kappa}} f(s'-\mathrm{i}\beta)\mathrm{d}s'\right)\right\}\mathrm{d}z. \tag{7.15}$$

Furthermore, the real part of the exponent in the integrand above can be expressed in the form

$$\mathrm{Re}\left\{-\mathrm{i}\mu^\alpha\int_0^{z/\tilde{\kappa}} f(s'-\mathrm{i}\beta)\mathrm{d}s'\right\} = 4\mu^\alpha\int_0^\infty \hat{f}(k)\frac{\sinh k\beta}{k}\sin^2\frac{z}{2\tilde{\kappa}}k\,\mathrm{d}k. \tag{7.16}$$

Thus, under the assumption $\hat{f}(k) \geq 0$ (satisfied by (i)–(iii) in Eq. (5.5) for $A > 0$) the right-hand side in Eq. (7.16) is positive; hence, the integral in Eq. (7.15) is exponentially large when $\mu \ll 1$ ($\mu^\alpha \gg 1$) and so is $\tilde{\kappa}\tilde{U}(\tilde{\kappa})/\Phi(0)$.

7.2. Radiating waves

From Eqs. (7.14) and (3.1), combined with $\hat{u}(-k) = \hat{u}(k)^*$, it follows that

$$\hat{u}(k) \sim \mp\frac{AC_-\exp\left(-\mu^\alpha(J_{-r}\pm\mathrm{i}J_{-i})\right)}{(A\Gamma(\alpha+1))^{\frac{1}{2(\alpha+1)}}}\sqrt{\frac{\alpha+1}{2\pi}}\frac{\mathrm{e}^{-\beta/\mu}}{\mu^{\alpha+1}}\frac{1}{k\mp 1/\mu} \quad (k \to \pm 1/\mu), \tag{7.17}$$

31

where $J_- = J_{-r} + \mathrm{i}J_{-i}$ was defined in Eq. (7.10). Then, upon inverting the Fourier transform $\hat{u}(k)$ as in Eq. (5.2), the poles in Eq. (7.17) contribute a radiating wave downstream in the form of Eq. (1.3), with

$$R = \frac{4\pi A C_-}{(A\Gamma(\alpha+1))^{\frac{1}{2(\alpha+1)}}} \sqrt{\frac{\alpha+1}{2\pi}} \frac{\exp(-\beta/\mu - \mu^\alpha J_{-r})}{\mu^{\alpha+1}}, \quad \theta = -\frac{\pi}{2} - \mu^\alpha J_{-i}.$$
(7.18)

It should be noted that in the small forcing-amplitude limit ($A \ll 1$), using the asymptotic expression (4.26) for C_- and $J_- \to 0$ in Eq. (7.18), we recover the linear wave response (viz., Eq. (5.4)).

According to Eq. (7.18), the main difference of the wave amplitude R from its linear counterpart R_{lin} (viz., Eq. (5.4)) is the $O(\mu^\alpha)$ modification of the exponent. This is a more significant nonlinear effect than those found earlier for $\alpha > 0$ (viz., Eq.(5.3)) and $\alpha = 0$ (viz., Eq.(6.26)): in view of the scaling $\varepsilon = \mu^{\alpha+1}$, decreasing the value of $\alpha (> -1)$ for fixed $\mu \ll 1$ effectively increases the nonlinearity parameter ε, so nonlinear effects are expected to be stronger. Furthermore, the extent to which nonlinearity affects the exponential factor in R hinges on (the sign and magnitude of) J_{-r} that depends on the specific forcing profile according to Eq. (7.10).

We have explored theoretically, based on Eq. (7.18), as well as numerically the effects of nonlinearity on the wave amplitude R when $-1 < \alpha < 0$ for the forcing profiles (i)–(iii) in Eq. (5.5). Figure 6 shows theoretical plots of $|R/R_{\mathrm{lin}}|$ as a function of $0 < A < 1$ for these forcings when $\alpha = -0.25$ and $\mu = 0.1, 0.2$ and 0.5. As before, the constant C_- was computed from the outer equation (4.1) by marching forward in κ and fitting $U(\kappa)$ as $\kappa \to 1$ to the exponential singularity predicted by dominant balance (viz., Eq. (4.8)). As a check, it was verified that when $A \ll 1$ the computed C_- agreed with the asymptotic expression (4.26). Furthermore, Fig. 6 shows numeri-

cal results of $|R/R_{\text{lin}}|$ computed by direct integration of the fKdV equation
(1.1) subject to the forcings (i)–(iii) for the same parameter values (with
$\varepsilon = \mu^{\alpha+1}$) as above. When $\mu = 0.2$ and 0.5, the theoretical predictions are
in satisfactory agreement with the numerical results for forcings (i) and (ii)
but not for (iii); in the latter case, while agreement does improve when μ is
reduced to 0.1, for $A \gtrsim 0.25$ the theory significantly overpredicts the wave
amplitude.

According to Fig. 6, nonlinearity causes the wave amplitude R to rise
sharply as the forcing amplitude A is increased, particularly for the forcings
(i) and (ii), where for $A \approx 0.5$ R has already reached ten times its linear
counterpart R_{lin}. Remarkably, this steep increase of R due to nonlinearity
for $\alpha = -0.25$ is noticeably stronger than that in Fig. 3 for $\alpha = 0$, even
though the forcing profiles differ relatively little for these two values of α.
The same trend also is seen upon comparing Fig. 7, which plots R as a
function of $A > 0$ for forcing (ii) and $\alpha = -0.25$ (with $\mu = 0.2$, 0.5), with
Fig. 4 which displays the corresponding response diagrams for $\alpha = 0$.

Finally, we remark that the agreement between theoretical predictions
(viz., Eq. (7.18)) and numerical results deteriorates when $\alpha \lesssim -0.3$. We have
made an attempt to remedy this difficulty by developing a more accurate
inner solution that accounts for the correction to the exponent of the singu-
larity of the outer solution for $\alpha < -1/2$ (viz., Eq. (4.17)). This modification
improves agreement with numerical results only to a limited extent: it turns
out that further corrections are needed when α drops below $-2/3$, $-4/5$,
$\cdots$. This hints that as α gets closer to -1 so $\varepsilon = \mu^{\alpha+1}$ approaches $O(1)$,
asymptotic treatment of the nonlinear wave response becomes a formidable
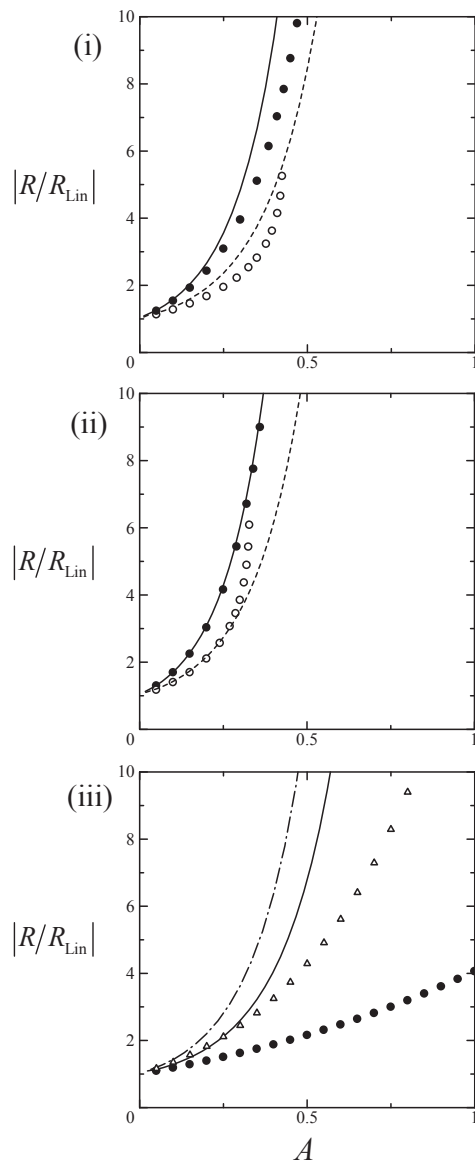task.

Figure 6: Ratio of nonlinear to linear wave amplitude as a function of the forcing amplitude A for $\alpha = -0.25$ with $\mu = 0.1$ (dash-dot line), 0.2 (solid line) and 0.5 (dashed line), corresponding to the forcing terms (i), (ii) and (iii) specified in Eq. (5.5). The circles (filled: $\mu = 0.2$, open: $\mu = 0.5$) and the open triangles ($\mu = 0.1$) are numerical results from direct integration of Eq. (1.1) subject to these forcing terms and $\varepsilon = \mu^{3/4}$.
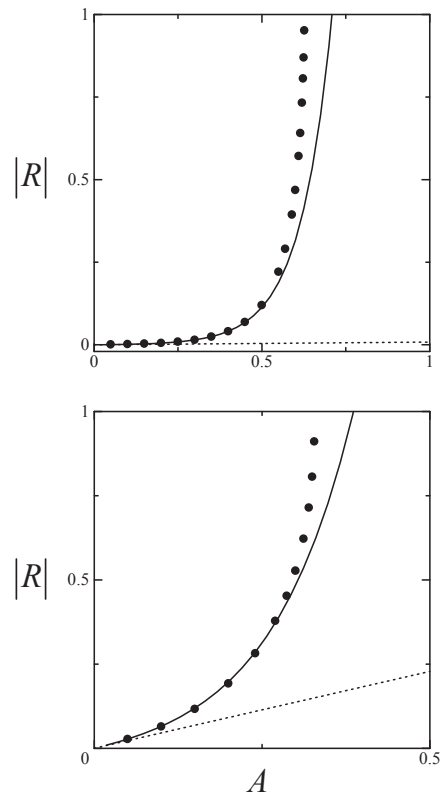
34

Figure 7: Wave amplitude $|R|$ as a function of the forcing amplitude A for the forcing term (ii) with $\alpha = -0.25$ specified in Eq. (5.5), with $\mu = 0.2$ (top) and 0.5 (bottom). The solid and dotted lines are nonlinear and linear responses, respectively. The circles denote numerical results from direct integration of Eq. (1.1) subject to this forcing term and $\varepsilon = \mu^{3/4}$.

8. Concluding remarks

Using the fKdV equation (1.1) as a simple model, we made an asymptotic study of nonlinear effects in steady radiating waves due to moving sources in dispersive media. In this model, the radiating wave amplitude is exponentially small with respect to the dispersion parameter $\mu \ll 1$. Yet, nonlinear effects (controlled by $\varepsilon \ll 1$) can play an important part, and computing the wave response for μ, $\varepsilon \ll 1$ may require the use of exponential (beyond-all-orders) asymptotics. In earlier studies, this issue was discussed for few examples of forcing profiles $f(x)$. Here, by contrast, we presented a systematic treatment of nonlinear wave responses due to even $f(x)$ with Fourier transform $\hat{f}(k)$ that decays for $|k| \gg 1$ like $A|k|^{\alpha} \exp(-\beta|k|)$, where A, α and $\beta > 0$ are free parameters.

For this class of forcing profiles, computing the radiating wave amplitude R and phase θ hinges upon beyond-all-orders asymptotics only if $\alpha > -1$. Under this condition, the appropriate scaling for nonlinear effects to come into play is $\varepsilon A = O(\mu^{\alpha+1})$. Furthermore, three distinct nonlinear responses arise depending on α: (i) $\alpha > 0$, (ii) $\alpha = 0$ and (iii) $-1 < \alpha < 0$. Specifically, taking $\varepsilon = \mu^{\alpha+1}$, the ratio of the nonlinear to the linear response amplitude for each of these cases is found to be: (i) $R/R_{\mathrm{lin}} = O(1)$ constant that depends on A and α; (ii) $R/R_{\mathrm{lin}} = O(1/\mu^A)$; and (iii) $R/R_{\mathrm{lin}} = O(\exp(A\mu^{\alpha}))$. The asymptotic expressions for R compare favorably against direct numerical solutions of the fKdV equation. Moreover, these comparisons suggest that the analytical predictions often remain reasonably accurate for moderate μ and ε, when the (formally exponentially small) wave amplitude can be quite substantial.

It should be noted that, in the limit $\alpha \to 0$, the radiated wave amplitude

formulae for $\alpha > 0$ (viz., Eq. (5.3)) and $\alpha < 0$ (viz., Eq. (7.18)) do not reduce to that for $\alpha = 0$ (viz., Eq. (6.26)). This suggests the need for a separate asymptotic theory that bridges the results for $\alpha > 0$ and $\alpha < 0$ in the neighborhood of $\alpha = 0$. The width of this neighborhood in terms of α and further details regarding this distinguished limit are not pursued here.

Finally, we comment on the wave response for $\alpha < -1$. In this instance, as suggested by Eq. (2.2), nonlinearity does not contribute to the disordering of expansion (2.1) so the scaling $\varepsilon A = O(\mu^{\alpha+1})$ is no longer relevant and the outer solution for $U(\kappa)$ is linear. However, when $\varepsilon A = O(\mu)$, nonlinearity does come into play in the vicinity of the simple pole at $\kappa = 1$ of the outer solution. Thus, to compute the residue of this pole, it is necessary to solve an inner equation for $\kappa = 1 + O(\mu)$, subject to matching with the (linear) outer solution.

Briefly, taking

$$\varepsilon = \mu \tag{8.1}$$

with $|A| \leq O(1)$, Eq. (3.7) for $U(\kappa)$ is replaced by

$$
\begin{aligned}
(1 - \kappa^2)U(\kappa) - 2\mu^{-\alpha}A \int_{\mu/\delta}^{\kappa/2} U(\lambda)U(\kappa - \lambda)\mathrm{d}\lambda \\
- 2\mu \int_{-\infty}^{1/\delta} \hat{f}(l)U(\kappa - \mu l)\,\mathrm{e}^{\beta l}\mathrm{d}l = \kappa^\alpha.
\end{aligned}
\tag{8.2}
$$

In the outer region, the nonlinear terms are subdominant and

$$U(\kappa) = \frac{\kappa^\alpha}{1 - \kappa^2}. \tag{8.3}$$

In the inner region, the appropriate variables are

$$U(\kappa) = \frac{\tilde{U}(\tilde{\kappa})}{\mu}, \quad \tilde{\kappa} = \frac{1 - \kappa}{\mu}, \tag{8.4}$$

and Eq. (8.2) yields, correct to $O(1)$,

$$\tilde{\kappa}\tilde{U}(\tilde{\kappa}) - \int_{-\infty}^{\infty} \hat{f}(l)\tilde{U}(\tilde{\kappa} - l)\,\mathrm{e}^{-\beta l}\mathrm{d}l = \frac{1}{2}. \tag{8.5}$$

37

The solution to the inner equation (8.5) is posed in the form of Eq. (6.4) subject to $\Phi(0) = -\mathrm{i}/2$. This condition ensures matching of the inner solution $\tilde{U}(\tilde{\kappa})$ when $\tilde{\kappa} \gg 1$ with the outer solution (8.3) when $\kappa \to 1$. Then, substituting Eq. (6.4) in Eq. (8.5), $\Phi(s)$ satisfies

$$\frac{\mathrm{d}\Phi}{\mathrm{d}s} + \mathrm{i}f(s - \mathrm{i}\beta)\Phi = 0 \tag{8.6}$$

so

$$\Phi(s) = -\frac{\mathrm{i}}{2} \exp\left\{-\mathrm{i}\int_0^s f(s' - \mathrm{i}\beta)\mathrm{d}s'\right\}, \tag{8.7}$$

and the inner solution is

$$\tilde{U}(\tilde{\kappa}) = -\frac{\mathrm{i}}{2}\int_0^\infty \exp\left\{\mathrm{i}\left(s\tilde{\kappa} - \int_0^s f(s' - \mathrm{i}\beta)\mathrm{d}s'\right)\right\}\mathrm{d}s. \tag{8.8}$$

As $\tilde{\kappa} \to 0$, we find from Eq. (8.8)

$$\tilde{U}(\tilde{\kappa}) \sim \frac{\mathrm{e}^{-J_-}}{2\tilde{\kappa}} \quad (\tilde{\kappa} \to 0), \tag{8.9}$$

where $J_- = J_{-r} + \mathrm{i}J_{-i}$ was defined in Eq. (7.10). In view of Eq. (8.4), this implies that the residue of the simple pole of $U(\kappa)$ at $\kappa = 1$ is $-\mathrm{e}^{-J_-}/2$. Thus, returning to Eq. (3.1) and also using $\hat{u}(-k) = \hat{u}^*(k)$, we may deduce the residues of the simple poles of $\hat{u}(k)$ at $k = \pm 1/\mu$:

$$\hat{u}(k) \sim \mp\frac{A}{2}\exp(-J_{-r} \mp \mathrm{i}J_{-i})\frac{\mathrm{e}^{-\beta/\mu}}{\mu^{\alpha+1}}\frac{1}{k \mp 1/\mu} \quad (k \to \pm 1/\mu). \tag{8.10}$$

Upon inverting the Fourier transform $\hat{u}(k)$ as in Eq. (5.2), these poles contribute a radiating wave downstream in the form of Eq. (1.3) with

$$R = 2\pi A\mathrm{e}^{-J_{-r}}\frac{\mathrm{e}^{-\beta/\mu}}{\mu^{\alpha+1}}, \qquad \theta = -\frac{\pi}{2} - J_{-i}. \tag{8.11}$$

Compared with the linear response (viz., Eq. (5.4)), the effects of nonlinearity on R and θ above are encapsulated in the $O(A)$ constant J_-, which is
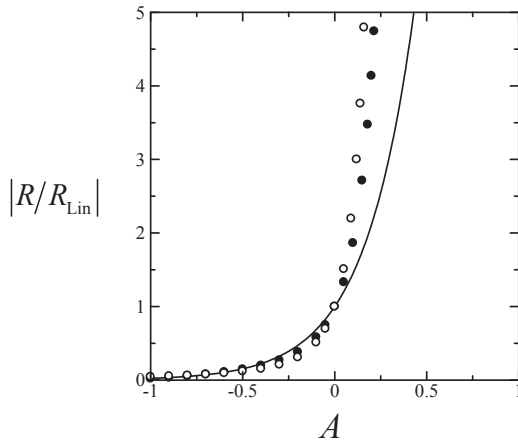
38

Figure 8: Ratio of nonlinear to linear wave amplitude as a function of the forcing amplitude A for the forcing (ii) with $\alpha = -2$ specified in Eq. (5.5). The filled ($\mu = 0.2$) and open ($\mu = 0.5$) circles are numerical results from direct integration of Eq. (1.1) subject to this forcing term and $\varepsilon = \mu$.

readily determined from the specific forcing profile (viz., Eq. (7.10)). Thus, unlike the nonlinear responses for $\alpha > -1$ treated earlier, here there is no need to resort to beyond-all-orders asymptotics.

Figure 8 plots $|R/R_{\text{lin}}| = \exp(-J_{-r})$ according to Eqs. (8.11) and (5.4), as a function of $-1 \leq A \leq 1$, for the forcing profile (ii) with $\alpha = -2$ in Eq. (5.5), along with numerical results from direct integration of the fKdV equation (1.1) for $\mu = 0.2$ and 0.5 (with $\varepsilon = \mu$). For these values of μ, there is overall good qualitative (as well as quantitative for $A \lesssim 0.25$) agreement between analytical and numerical results. As also found earlier for $\alpha \geq 0$ (see Figs. 1–3), the main effect of nonlinearity is to dramatically increase (decrease) the response amplitude when $A > 0$ ($A < 0$).

Acknowledgements

Appendix A. Higher-order analysis for $\alpha > 0$

In Section 4.1 it was argued that for $\alpha > 0$ the outer analysis is sufficient to compute asymptotically the radiating waves downstream. This leading-order approximation was compared with numerical results for the forcing terms (i)–(iii) in Eq. (5.5) that satisfy the assumed asymptotic behavior in Eq. (1.7). However, for the (moderately small) values of $\mu = 0.1$ and 0.2, good quantitative agreement between analytical and numerical results was found only for (i) and (ii) (see Fig. 1). To remedy this difficulty, here we present a higher-order analysis that takes into account, via an inner solution, the effect of the second integral in Eq. (3.7), which formally is subdominant and was dropped earlier. This inner solution is similar to that obtained for $\alpha = 0$ in Section 6.1 and only the main steps are highlighted below.

Similar to Eq. (6.1), using the inner variables

$$U(\kappa) = \frac{\tilde{U}(\tilde{\kappa})}{\mu}, \qquad \tilde{\kappa} = \frac{1 - \kappa}{\mu}, \tag{A.1}$$

the first derivative of Eq. (3.7) is approximated correct to $O(\mu^{\alpha-1})$ by the inner equation

$$\tilde{\kappa}\tilde{U}'(\tilde{\kappa}) + \tilde{U}(\tilde{\kappa}) - \mu^{\alpha} \int_{-\infty}^{\infty} \hat{f}(l)\tilde{U}'(\tilde{\kappa} - l)\,e^{-\beta l}\mathrm{d}l = 0, \tag{A.2}$$

where prime indicates derivative with respect to $\tilde{\kappa}$. (This assumes $0 < \alpha < 1$. To derive the appropriate inner equation for $\alpha \geq 1$, it is necessary to work with a higher derivative of Eq. (3.7), but the final results in Eq. (A.12) are not changed.)

The solution to Eq. (A.2) is posed in the same form as Eq. (6.4), and $\Phi(s)$ satisfies

$$\frac{\mathrm{d}\Phi}{\mathrm{d}s} + \mathrm{i}\mu^\alpha f(s - \mathrm{i}\beta)\,\Phi = 0, \tag{A.3}$$

under the assumption that $s\Phi(s) \to 0$ as $s \to 0$ (to be verified below). Therefore,

$$\Phi = \tilde{C}_+ \exp\left\{\mathrm{i}\mu^\alpha \int_s^\infty f(s' - \mathrm{i}\beta)\mathrm{d}s'\right\}, \tag{A.4}$$

where $\tilde{C}_+$ is a constant that is specified by matching with the outer solution. It should be noted that

$$f(s - \mathrm{i}\beta) \sim \left(\frac{\mathrm{i}}{s}\right)^{\alpha+1} A\Gamma(\alpha + 1) \quad (s \to 0), \tag{A.5}$$

so $s\Phi(s) \sim \tilde{C}_+ s \exp\left\{-(\mathrm{i}\mu/s)^\alpha A\Gamma(\alpha)\right\} \to 0$ as $s \to 0$ (with $\mu \ll s \ll 1$). Then, inserting (A.4) in Eq. (6.4) yields the inner solution

$$\tilde{U}(\tilde{\kappa}) = \tilde{C}_+ \int_0^\infty \exp\left\{\mathrm{i}\left(s\tilde{\kappa} + \mu^\alpha \int_s^\infty f(s' - \mathrm{i}\beta)\mathrm{d}s'\right)\right\}\mathrm{d}s. \tag{A.6}$$

From Eq. (A.6), we find that

$$\tilde{U}(\tilde{\kappa}) \sim \mathrm{i}\frac{\tilde{C}_+}{\tilde{\kappa}} \quad (\tilde{\kappa} \to 0). \tag{A.7}$$

Furthermore, the outer limit of Eq. (A.6) is

$$\tilde{U}(\tilde{\kappa}) \sim \mathrm{i}\tilde{C}_+ \frac{\mathrm{e}^{\mu^\alpha J_+}}{\tilde{\kappa}} \quad (1 \ll \tilde{\kappa} \ll 1/\mu), \tag{A.8}$$

where

$$J_+ = \mathrm{i} \int_0^\infty \left\{f(s - \mathrm{i}\beta) - \left(\frac{\mathrm{i}}{s}\right)^{\alpha+1} A\Gamma(\alpha + 1)\right\}\mathrm{d}s. \tag{A.9}$$

Thus, matching of the outer limit of the inner solution in Eq. (A.8) with the inner limit $(\kappa \to 1)$ of the outer solution in Eq. (4.4) is achieved if

$$\tilde{C}_+ = -\mathrm{i}\mathrm{e}^{-\mu^\alpha J_+} C. \tag{A.10}$$

41

Finally, combining Eqs. (A.10), (A.7) and (A.1) with Eq. (3.1), we conclude that

$$\hat{u}(k) \sim \mp AC \exp(-\mu^\alpha (J_{+r} \pm \mathrm{i} J_{+i})) \frac{\mathrm{e}^{-\beta/\mu}}{\mu^{\alpha+1}} \frac{1}{k \mp 1/\mu} \quad (k \to \pm 1/\mu). \quad \text{(A.11)}$$

Upon inverting $\hat{u}(k)$, these residues contribute a radiating wave downsream in the form of Eq. (1.3) with

$$R = 4\pi AC \frac{\exp(-\beta/\mu - \mu^\alpha J_{+r})}{\mu^{\alpha+1}}, \quad \theta = -\frac{\pi}{2} - \mu^\alpha J_{+i}, \quad \text{(A.12)}$$

where $J_+ = J_{+r} + \mathrm{i} J_{+i}$ was defined in (A.9).

Unlike the leading-order result in Eq. (5.3), based on the refined expression for R in Eq. (A.12) the ratio of the nonlinear to the linear response amplitude $|R/R_{\mathrm{lin}}|$ now depends on μ. As shown in Fig. 2, this modification greatly improves the agreement between analytical and numerical results for the forcing term (iii) and $\mu = 0.1$, 0.2.

References

[1] P. G. Baines, Topographic Effects in Stratified Flows, Cambridge University Press, 1995.

[2] J. N. Newman, Marine Hydrodynamics, MIT Press, 1977.

[3] G. B. Whitham, Linear and Nonlinear Waves, Wiley Interscience, 1974.

[4] M. J. Lighthill, Waves in Fluids, Cambridge University Press, 1978.

[5] G. Dagan, Waves and wave resistance of thin bodies moving at low speed: the free-surface nonlinear effect, J. Fluid Mech. 69 (1975) 405–416.

[6] G. Dagan, T. Miloh, A study of nonlinear wave resistance by a Zakharov-type integral equation, In: Proc. 15th Symp. Naval Hydrodynamics, Hamburg (1985) 373–386.

[7] T. R. Akylas, T.-S. Yang, On short-scale oscillatory tails of long-wave disturbances, Stud. Appl. Math. 94 (1995) 1–20.

[8] T.-S. Yang, T. R. Akylas, Finite-amplitude effects on steady lee-wave patterns in subcritical stratified flow over topography, J. Fluid Mech. 308 (1996) 147–170.

[9] R. Grimshaw, Exponential asymptotics and generalized solitary waves, In: Asymptotic Methods in Fluid Mechanics: Survey and Recent Advances (edited by H. Steinrück), CISM Courses and Lectures, Springer (2010) 71–120.

[10] J. P. Boyd, Weakly Nonlocal Solitary Waves and Beyond-All-Orders Asymptotics, Springer, 1998.

[11] S. D. Nixon, T. R. Akylas, J. Yang, New aspects of exponential asymptotics in multiple-scale nonlinear wave problems, Stud. Appl. Math. 139 (2017) 223–247.

[12] C. M. Bender, S. A. Orszag, Advanced Mathematical Methods for Scientists and Engineers, McGraw-Hill, 1978.